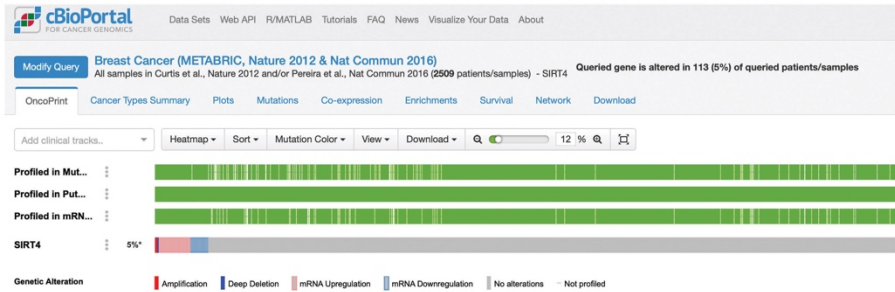


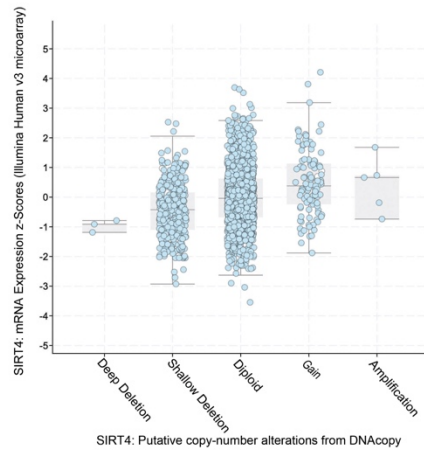
Supplementary Figures and Figure legends

Figure S1 Related to Figure 1

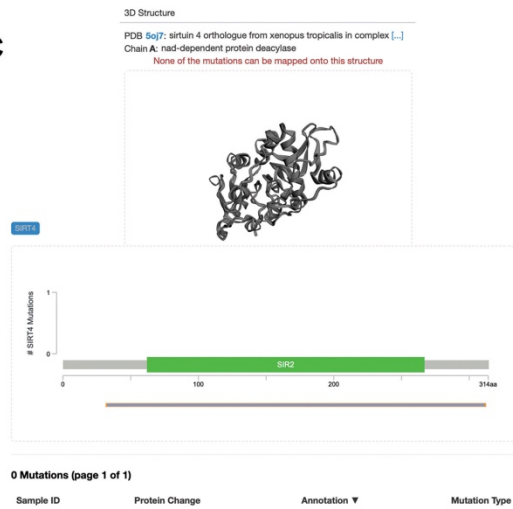
A



B



C



D

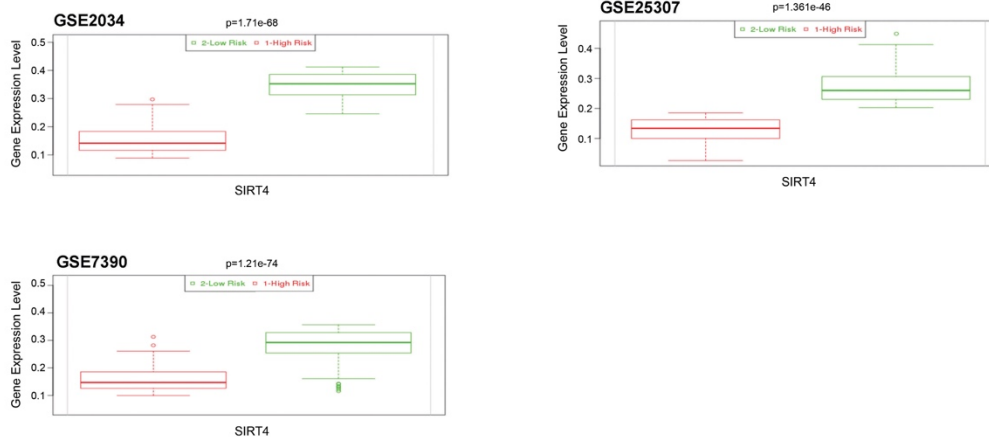


Figure S1. (A) TCGA database available from cBioportal for SIRT4 expression in human breast cancers. (B) Copy number compared to gene expression for SIRT4 mRNA versus copy number in human breast cancers using the cBioportal database. (C) Putative 3D structures of SIRT4 protein generated from the cBioportal database. (D)

Gene expression of SIRT4 in human breast cancer compared to normal tissues from 3 Gene Expression Omnibus (GEO) data sets (GSE2034, 25307, 7390).

Figure S2 Related to Figure 1

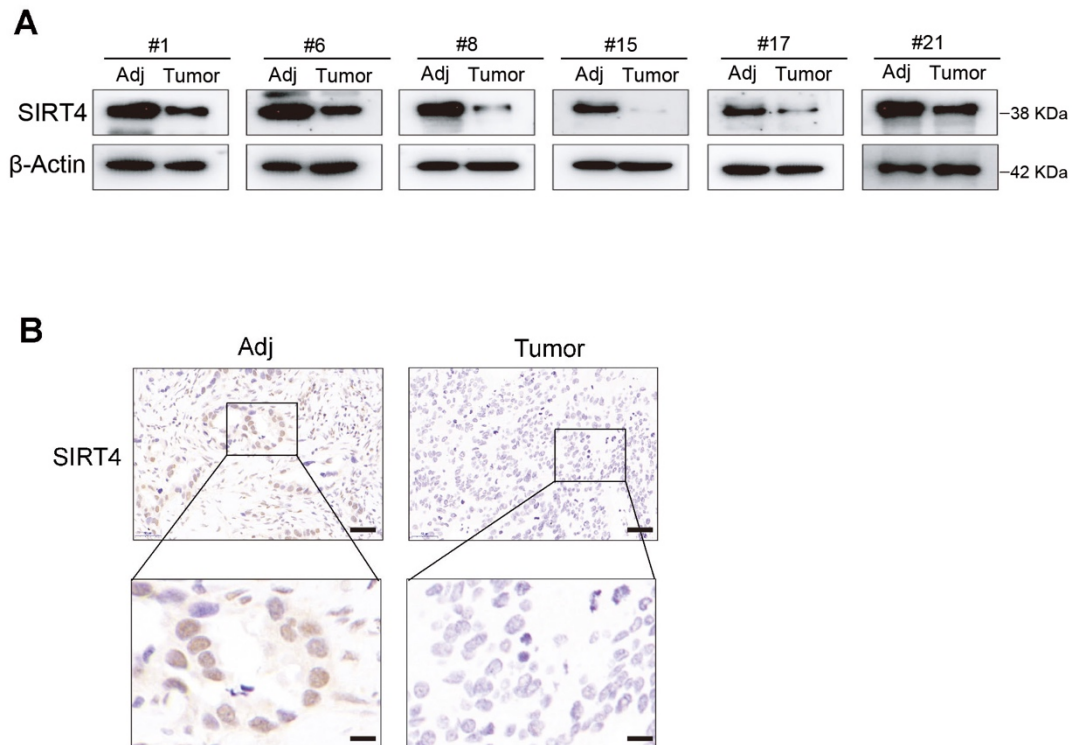


Figure S2. (A) Immunoblotting of SIRT4 in breast tumors compared to normal tissues (n=6). (B) Representative IHC staining images of SIRT4 in breast tumors compared to normal tissues; Scale bars, 100 μ m (B) and 20 μ m in the insets (B).

Figure S3 Related to Figure 1

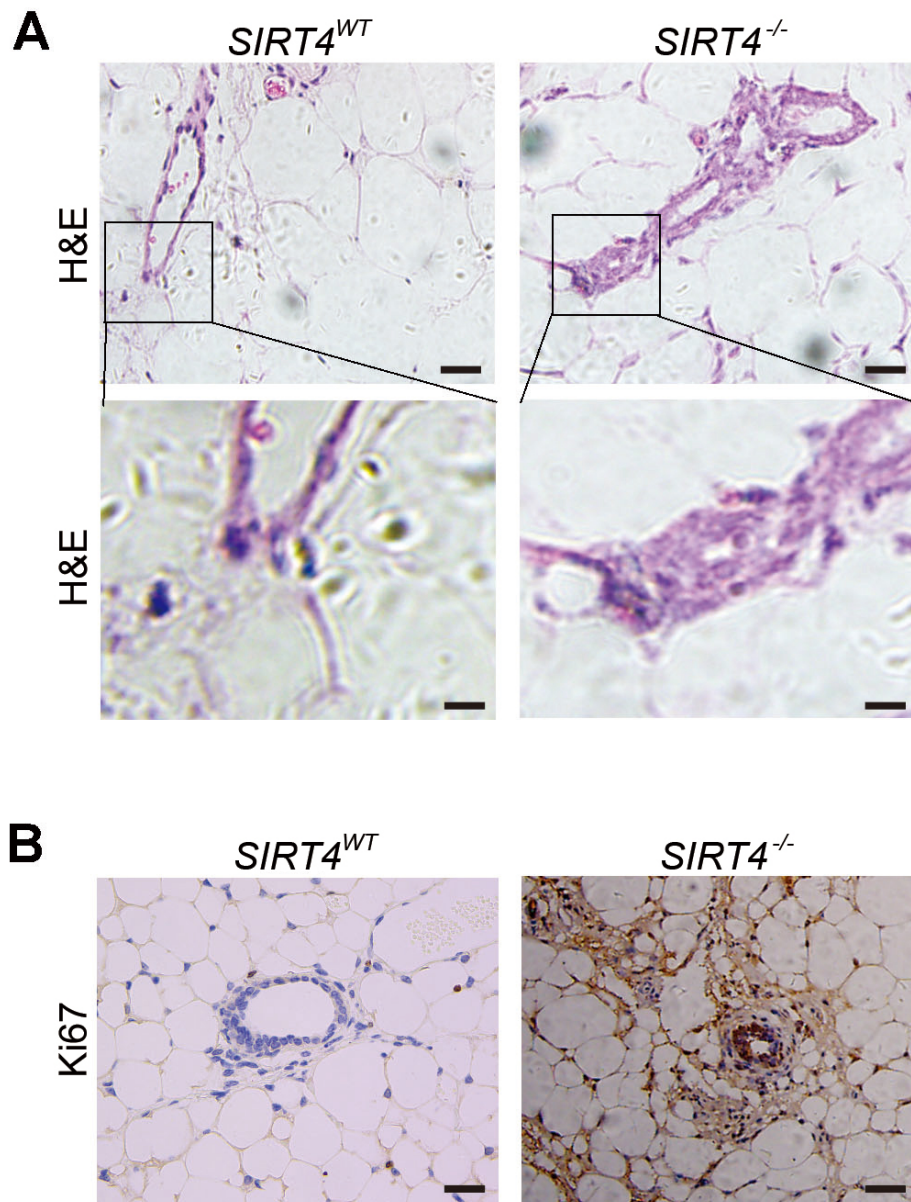


Figure S3. Representative H&E staining (A) and IHC staining images of Ki67 (B) for sections of mammary glands isolated from *SIRT4^{WT}* and *SIRT4^{-/-}* mice; Scale bars, 100 μm (A) and 20 μm in the insets (A), 100 μm (B).

Figure S4 Related to Figure 2

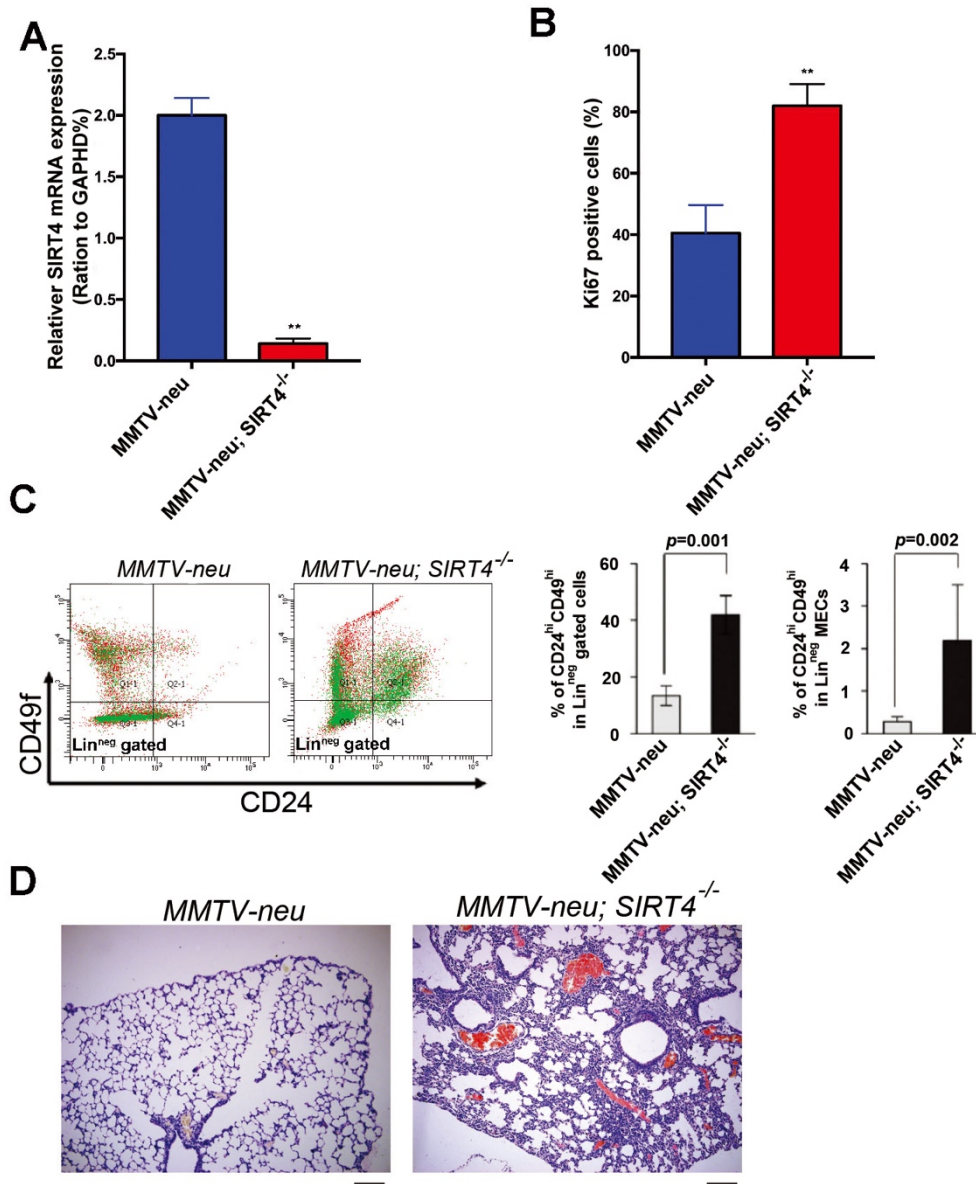


Figure S4. (A) mRNA expression of SIRT4 in tumors isolated from MMTV-neu and MMTV-neu; SIRT4^{-/-} mice. (B) Quantification of Fig.2E. (C) Distribution of Lin^{neg} mouse mammary cells according to their expression of CD24 and CD49f were analyzed on MMTV-neu and MMTV-neu; SIRT4^{-/-} mice (left) and its quantification (right). (D) Representative H&E staining images for sections of lung metastasis isolated from mice mentioned above; Scale bars, 200 μ m (D).

Figure S5 Related to Figure 3

SIRT4^{-/-} *SIRT4*^{WT}

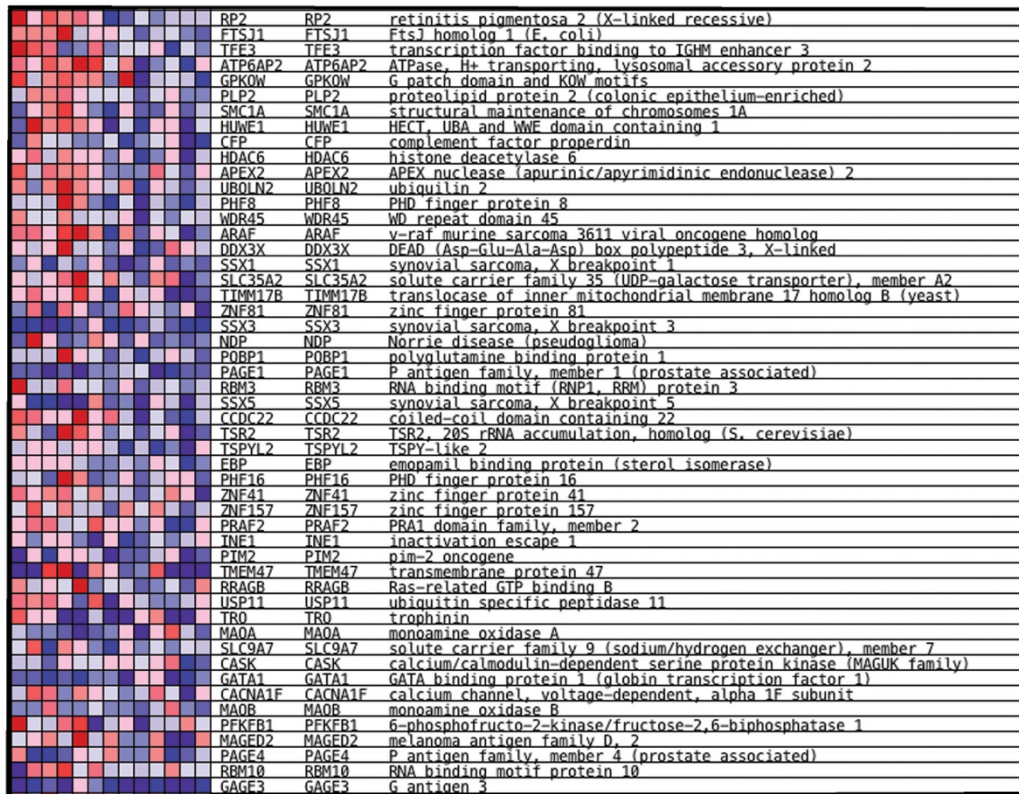


Figure S5. Top 50 of the genes displayed in Fig.3A.

Figure S6 Related to Figure 3

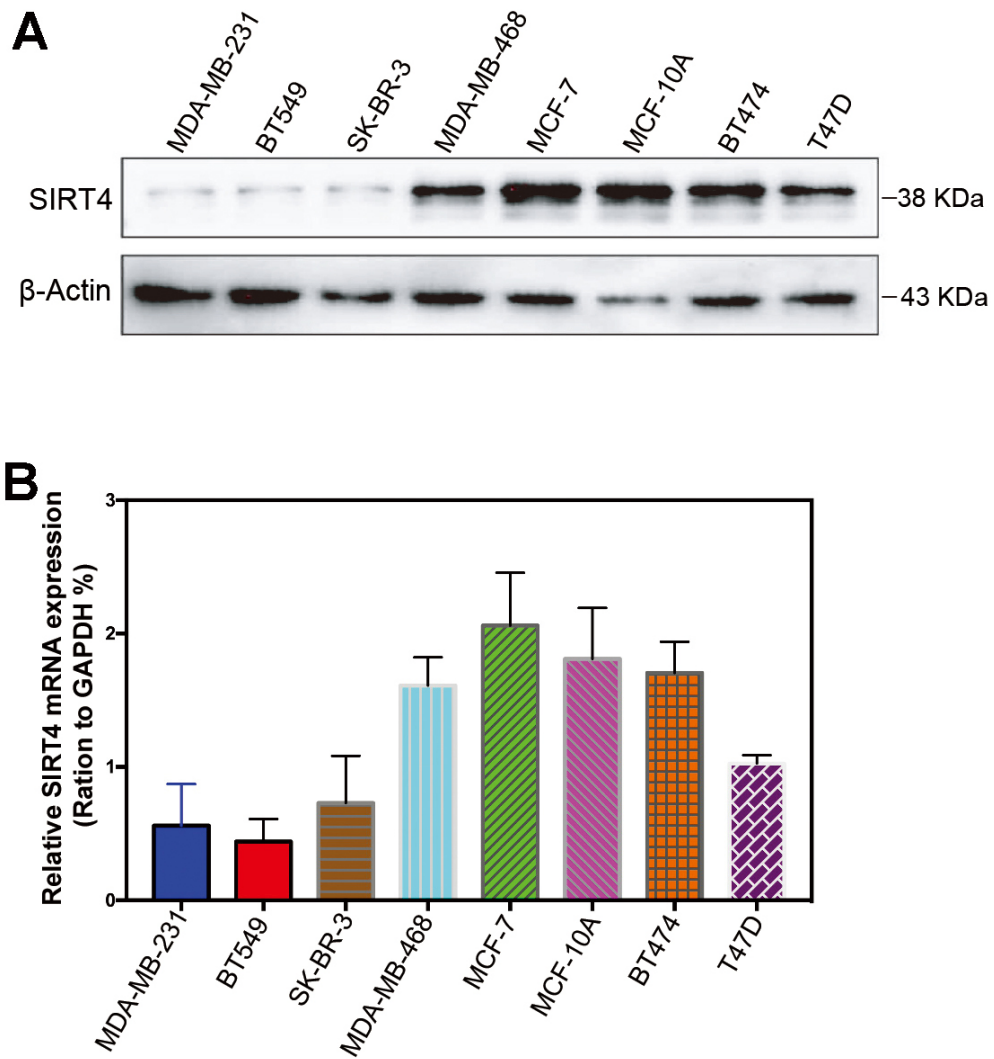


Figure S6. Immunoblotting (A) and mRNA expression (B) of SIRT4 among breast cancer cell lines.

Figure S7 Related to Figure 3

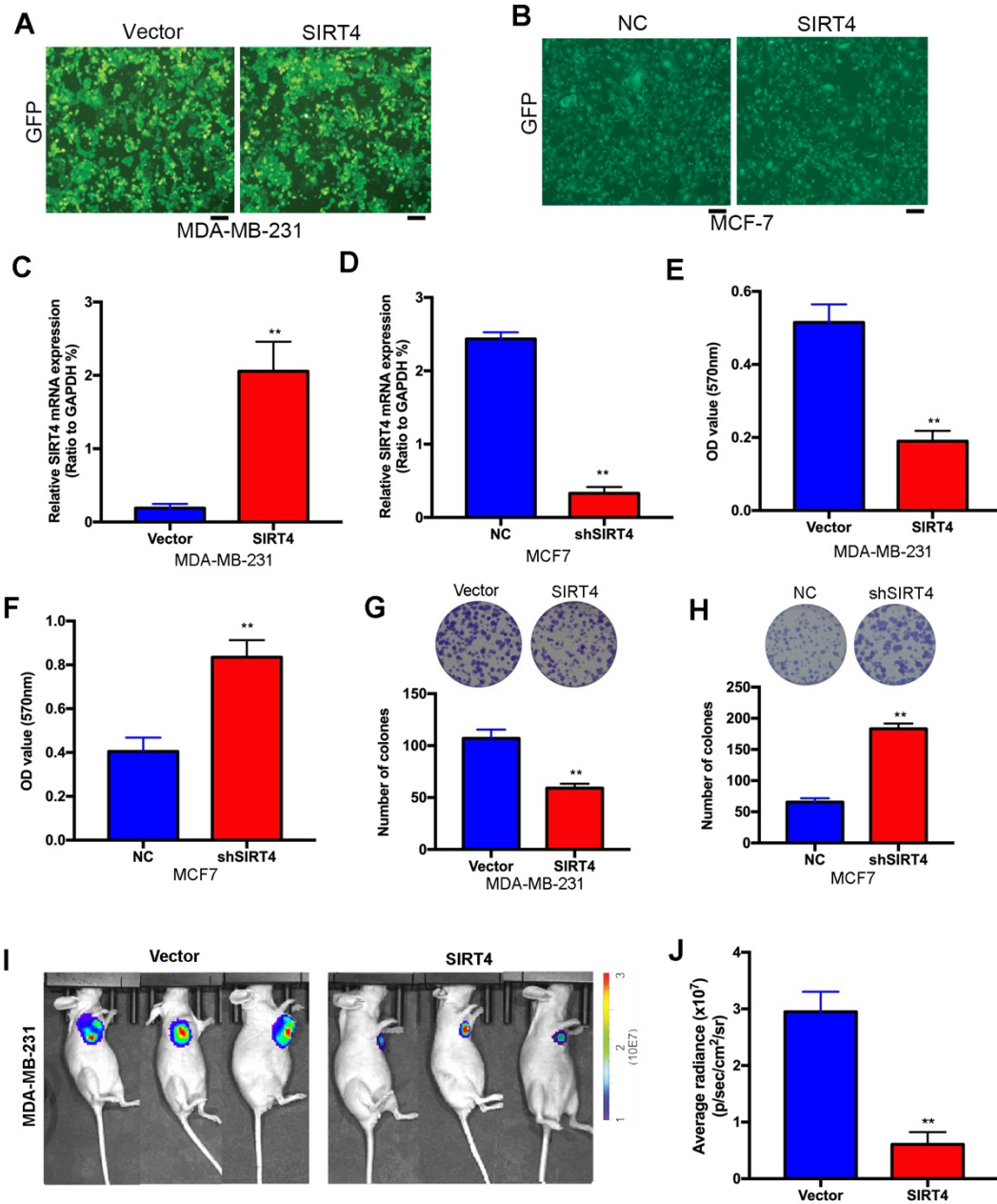


Figure S7. (A-D) Transfection efficiency of MDA-MB-231 (A, C) and MCF-7 cells (B, D) transfected with control vector, SIRT4, and/or sh-SIRT4 measured by GFP (A, B) or mRNA expression (C, D). **(E-H)** In vitro MTT (E, F) and sphere formation assay (G, H) with transformed MDA-MB-231 (E, G) and MCF-7 cells (F, H) described above. **(I, J)** Representative ventral view images of bioluminescence from mice (n=3) with injections of MDA-MB-231 cells described above (I) and its quantification (J).

Figure S8 Related to Figure 3

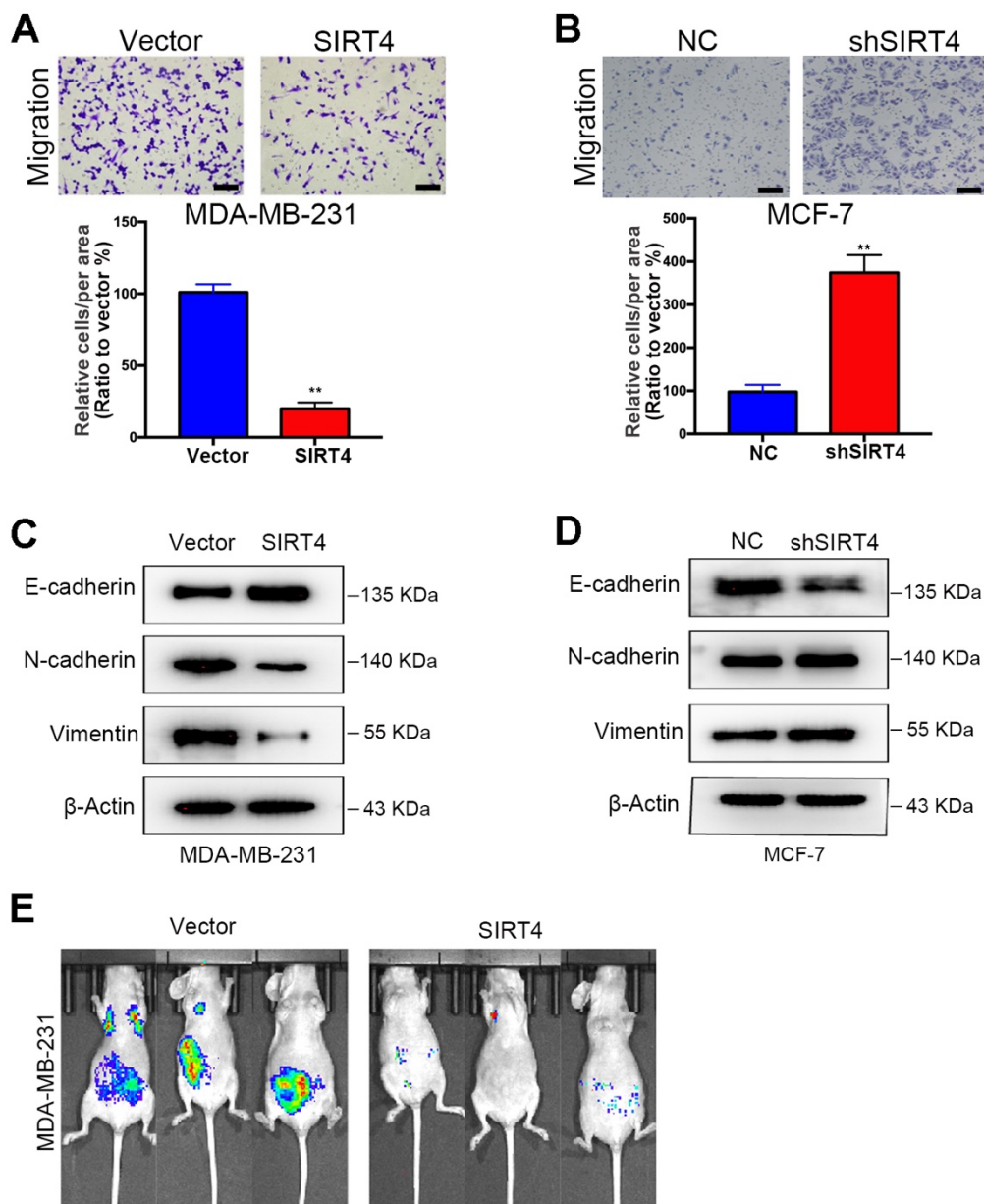


Figure S8. (A, B) Migration assay (upper) and its quantification (bottom) of transformed MDA-MB-231 (A) and MCF-7 cells (B) described in Supplementary Figure 8. (C, D) Immunoblotting of transformed MDA-MB-231 (C) and MCF-7 cells (D) described above. (E) Representative ventral view images of bioluminescence from mice (n=3) with injections of MDA-MB-231 cells described above; Scale bars, 100 μ m (A) and 100 μ m (B).

Figure S9 Related to Figure 4

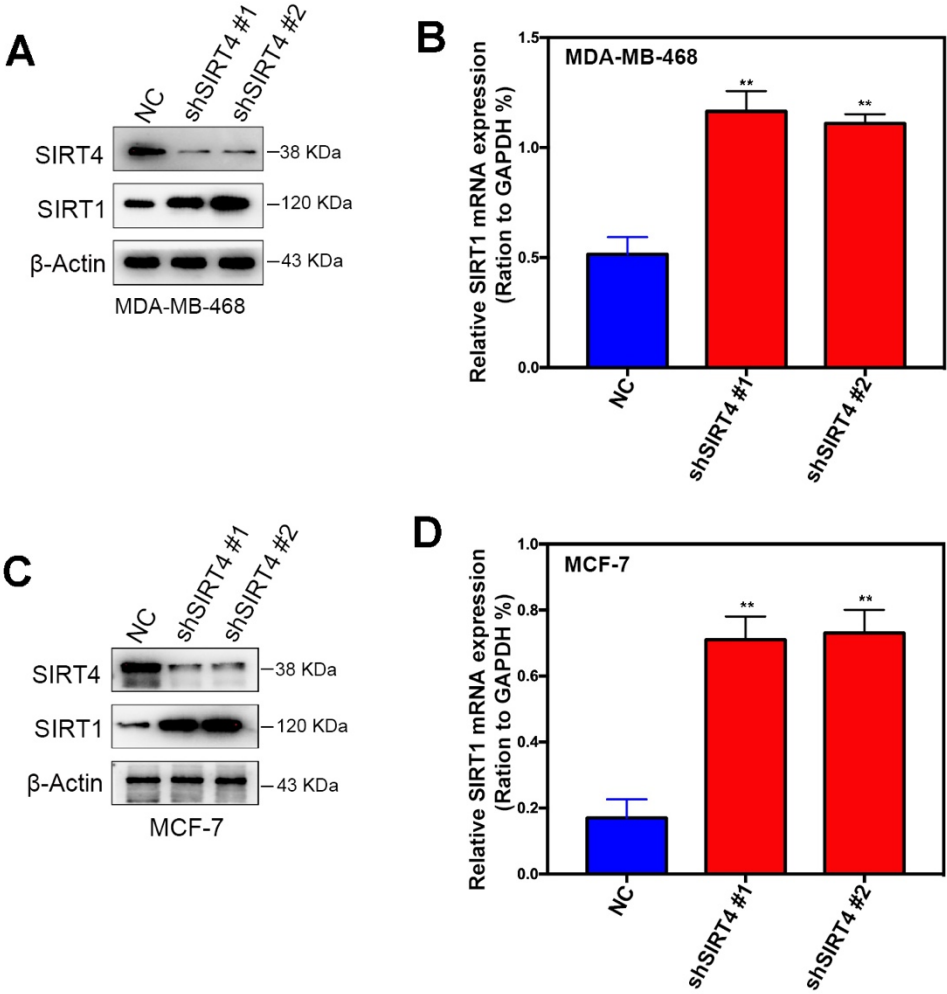


Figure S9. Immunoblotting (A, C) and mRNA (B, D) expression of SIRT4 and SIRT1 in transformed MDA-MB-468 (A, B) and MCF-7 cells (C, D) described in Fig.3G.

Figure S10 Related to Figure 4

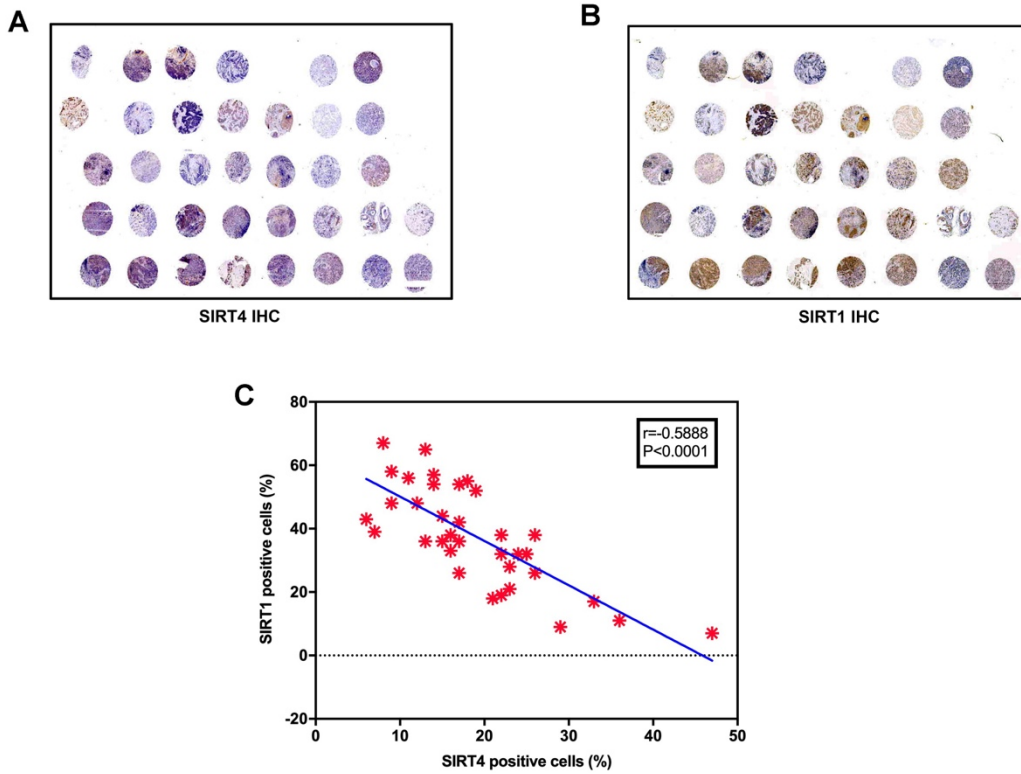


Figure S10. (A, B) Representative IHC staining images of SIRT4 (A) and SIRT1 (B) in mammary tissues from 36 breast cancer patients. (B) Quantification of (A, B). (C) Negative association between SIRT4 and SIRT1 protein expression in breast tumor tissues.

Figure S11 Related to Figure 5

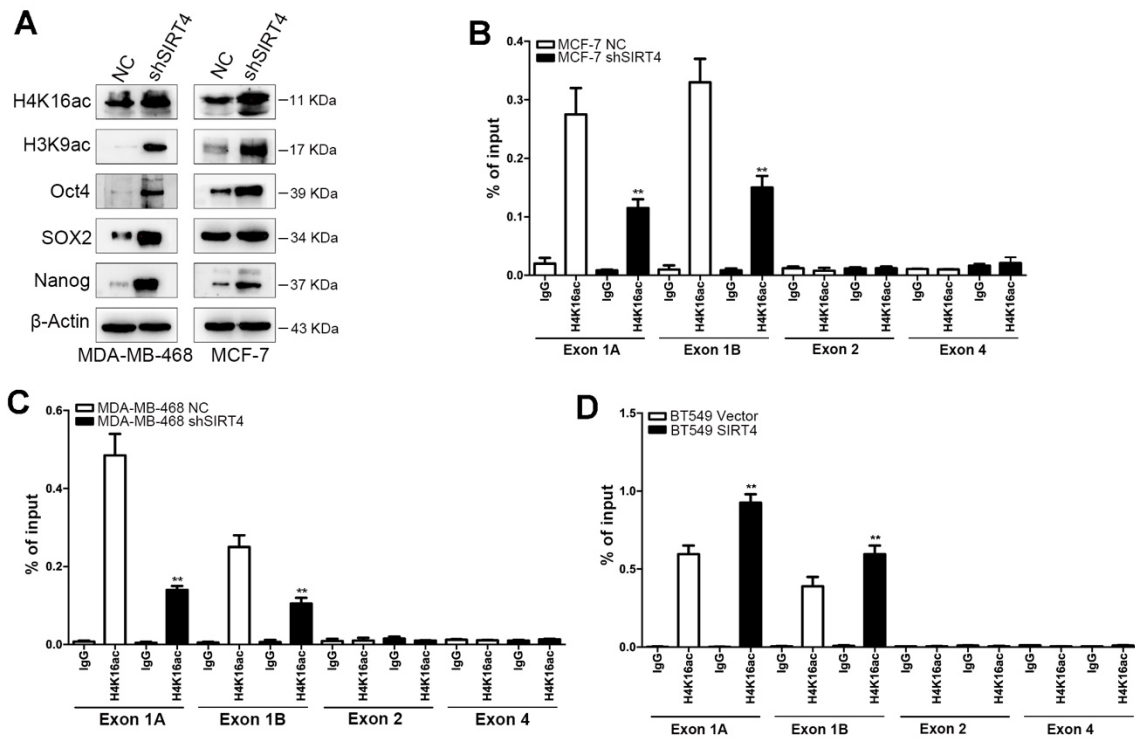


Figure S11. (A) Immunoblotting of acetyl-histone H4 at lys16 (H4K16ac), acetyl-histone H3 at lys9 (H3K9ac), Oct4, SOX2, and Nanog in MDA-MB-468 (left panel) as well as MCF-7 cells (right panel) transfected with control (NC) or shSIRT4 vector. (B-D) transformed MCF-7 (B), MDA-MB-231 (C), and BT549 cells (D) as described in Fig.3 were chromatin immunoprecipitated for IgG and H4K16ac. Pull-down at the putative H4K16ac binding sites was assessed by qRT-PCR and calculated as percent of IgG input. Error bars are SEM for 3 technical replicates.

Figure S12 Related to Figure 5

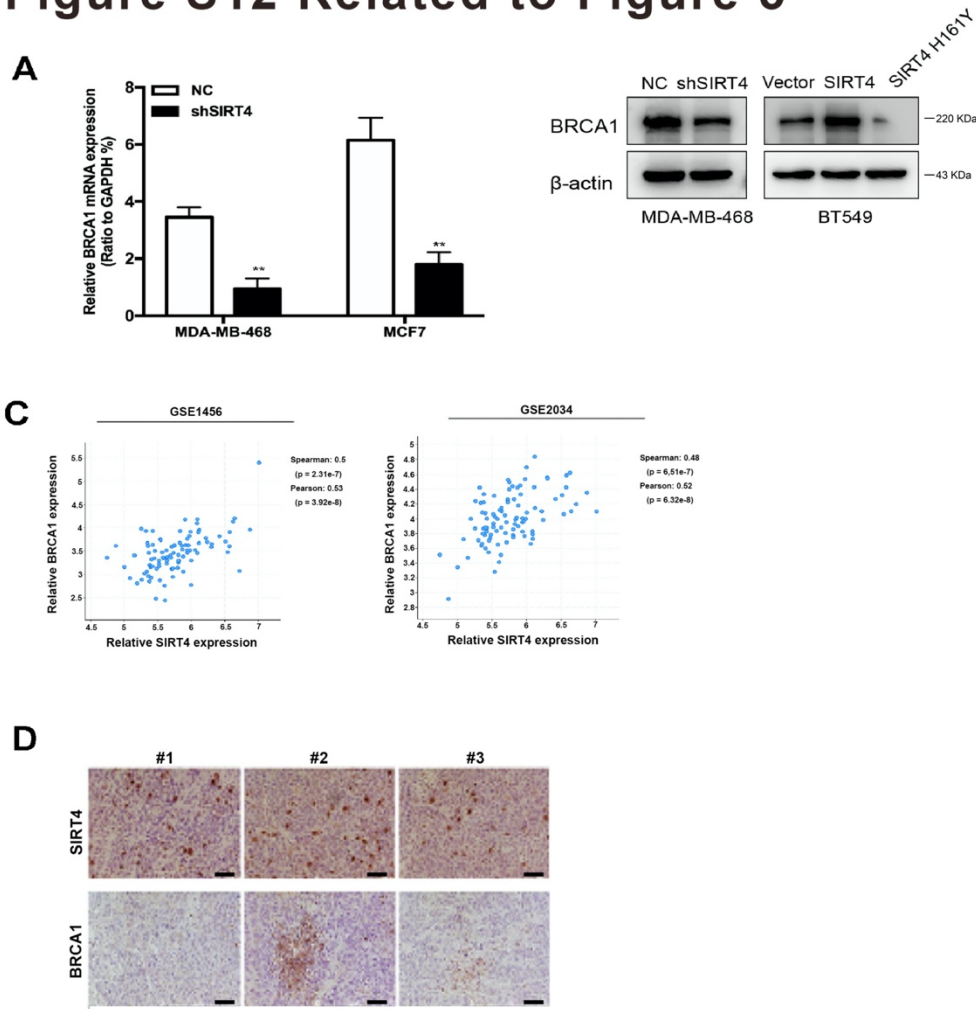


Figure S12. (A, B, C) Immunoblotting (B) and mRNA expression (C) of BRCA1 in MDA-MB-468, MCF7 and BT579 cells describe in Fig5. (D) Reverse relationship between SIRT4 and BRCA1 generated from 3 databases (GSE1456, 2034, and 4922). (E) Representative IHC staining images of SIRT4 and BRCA1 in tumor sections isolated from human mammary tissues; Scale bars, 100 μ m (D).

Figure S13 Related to Figure 6

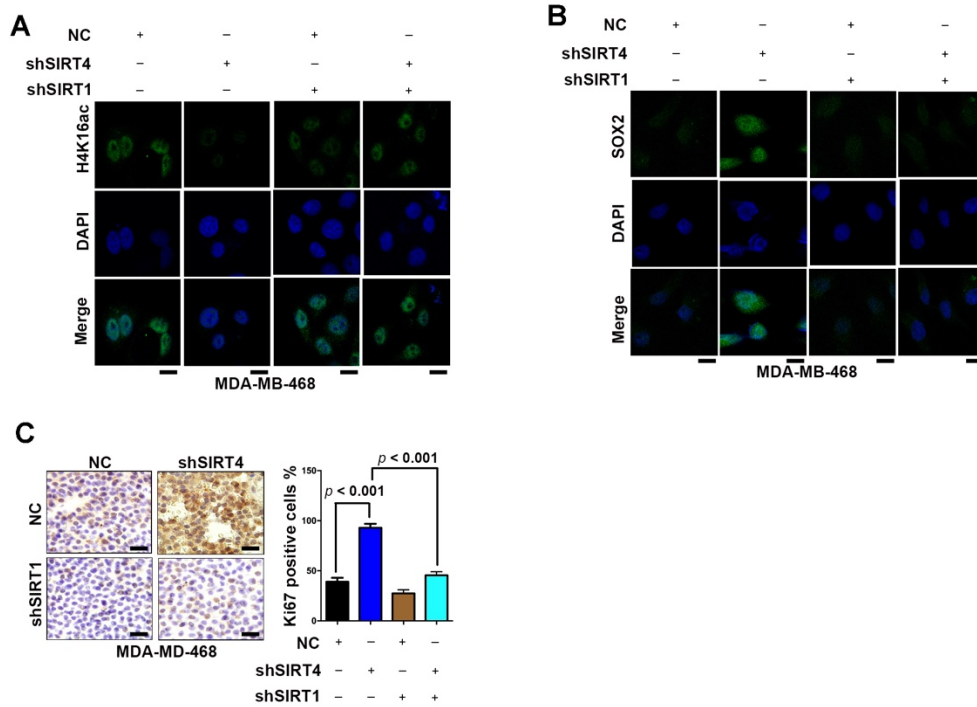


Figure S13. (A, B) Immunofluorescence images of MDA-MB-468 cells described in Fig.6A stained with antibodies against H4K16ac/DAPI (A) and SOX2/DAPI (B). **(C)** Representative IHC staining images (left) and its quantification (right) of Ki67 in MDA-MB-468 cells described above; Scale bars, 20 μ m (A) and 20 μ m (B).

Figure S14 Related to Figure 7

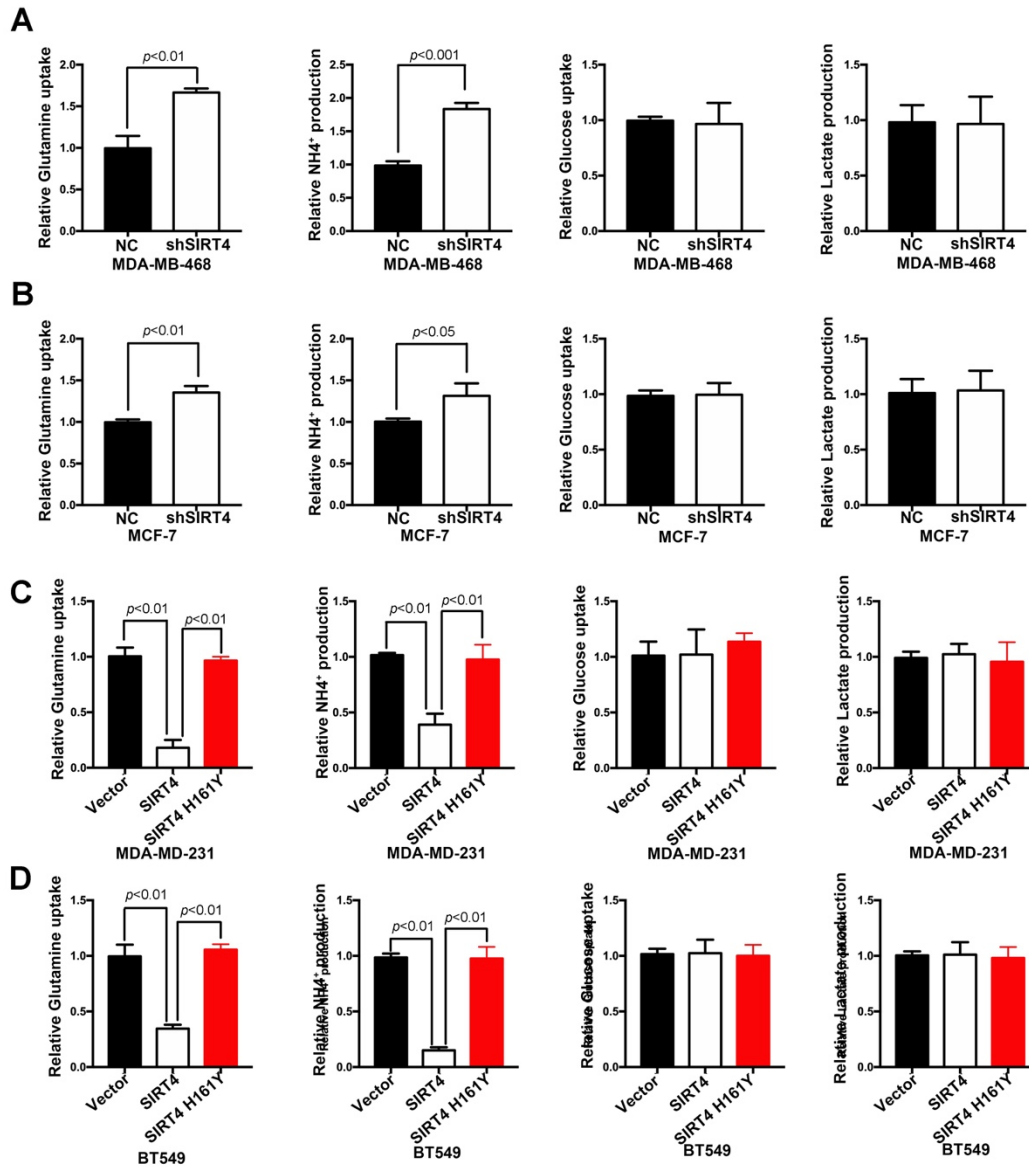


Figure S14. (A-D) Measurement of Glutamine uptake, NH₄⁺ production, Glucose uptake, and lactate production (from left to right panel) in MDA-MB-468 (A), MCF-7 (B), MDA-MB-231 (C), and BT549 (D) cells.

Figure S15 Related to Figure 7

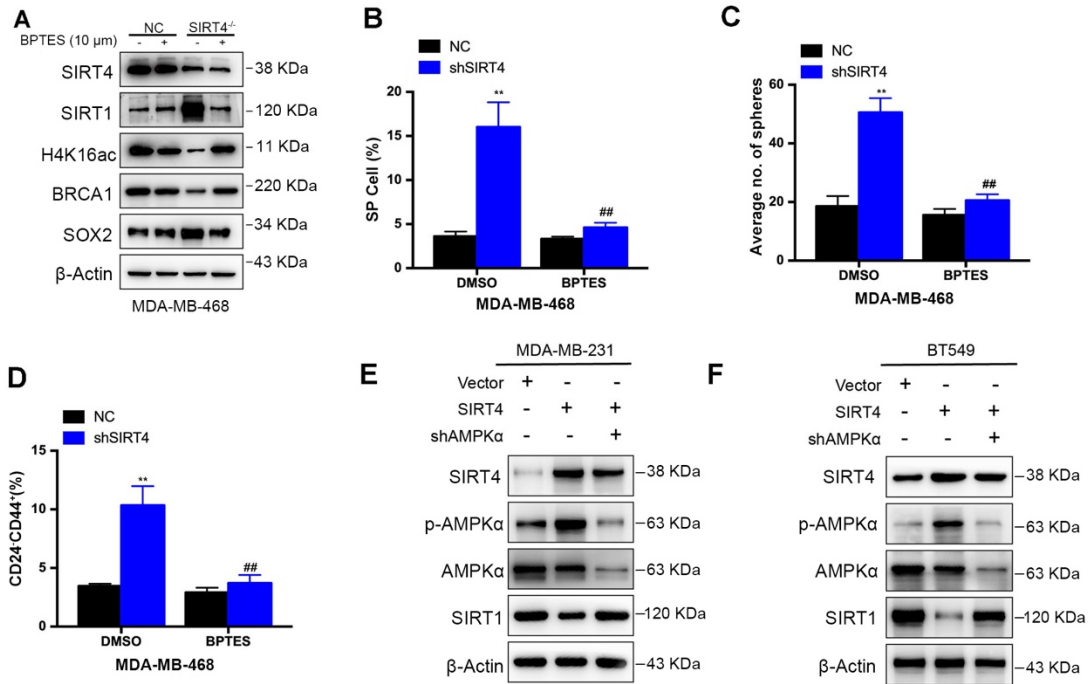


Figure S15. (A) Immunoblotting of indicated proteins isolated from MDA-MB-468 cells with or without BPTES (10 μ M) treatment. (B, C, D) Quantification of Hoechst SP assay (B), sphere formation efficiency (C), and CD44⁺/CD24⁻ subpopulations (D) in MDA-MB-468 cells with or without BPTES treatment.

Full unedited gel for western blots figures

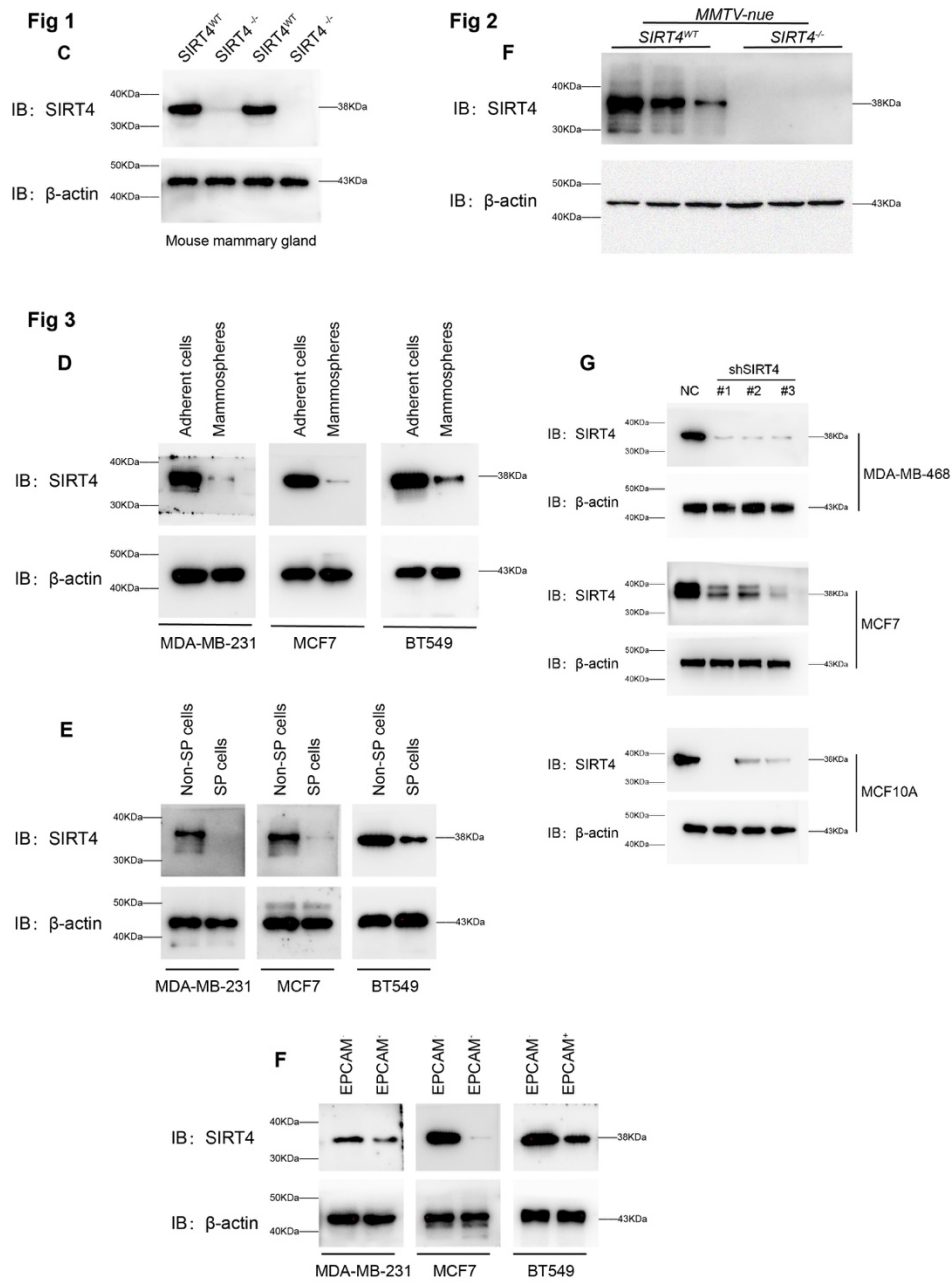


Fig 3
H

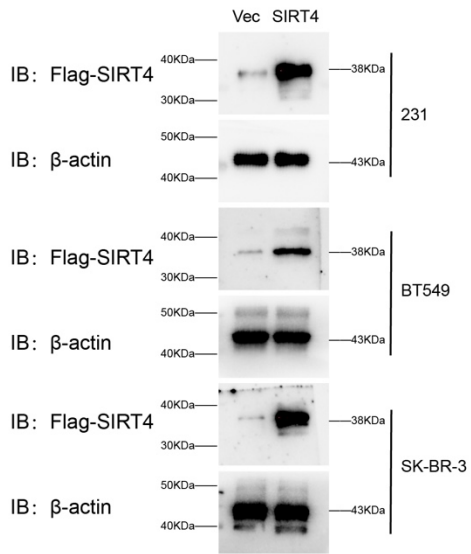
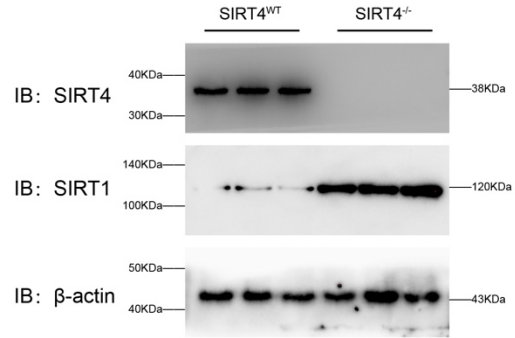


Fig 4
E



F

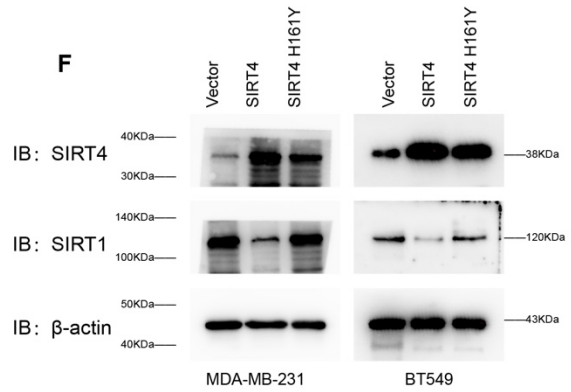


Fig 5

A

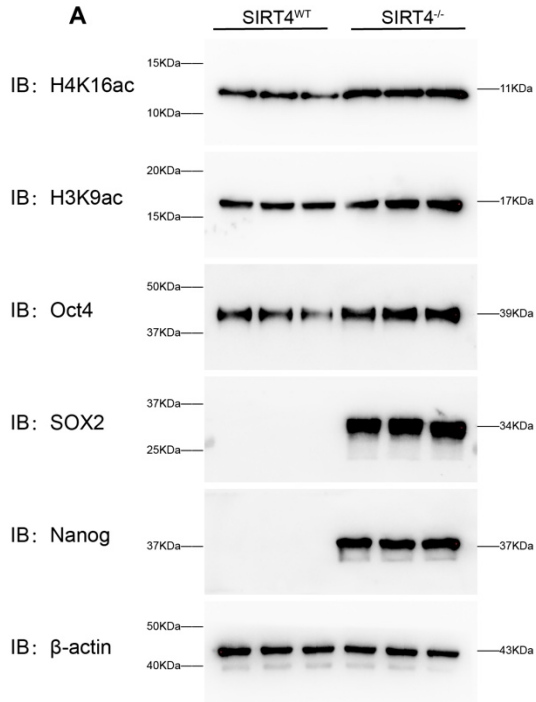


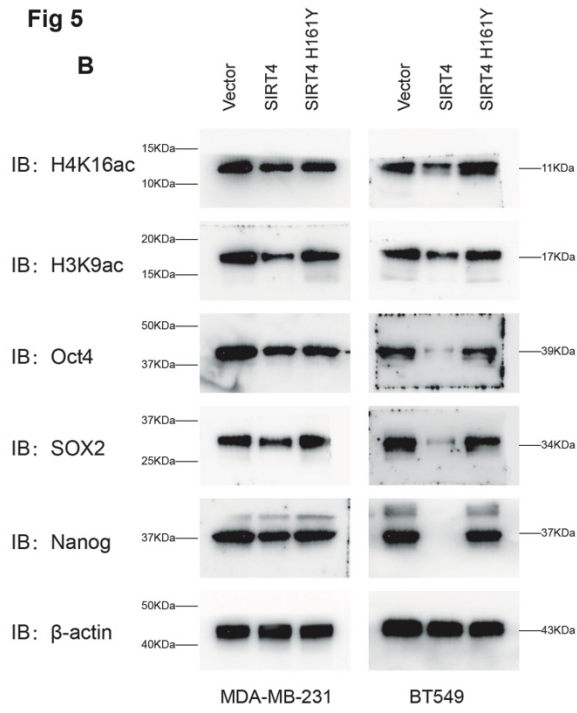
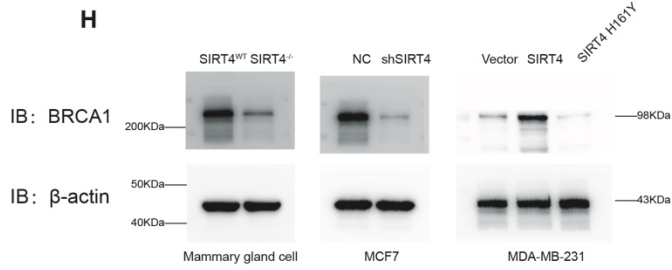
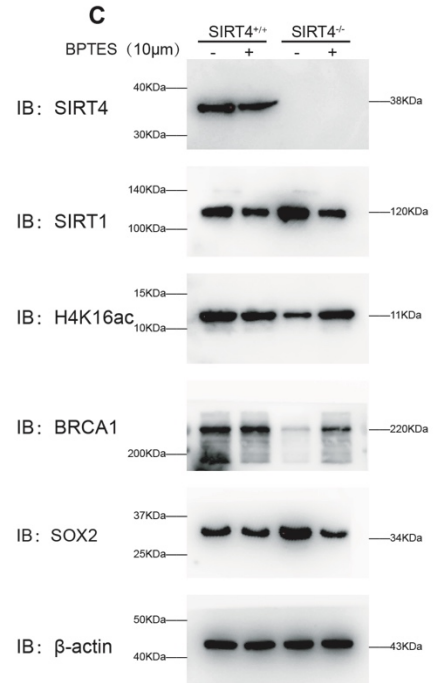
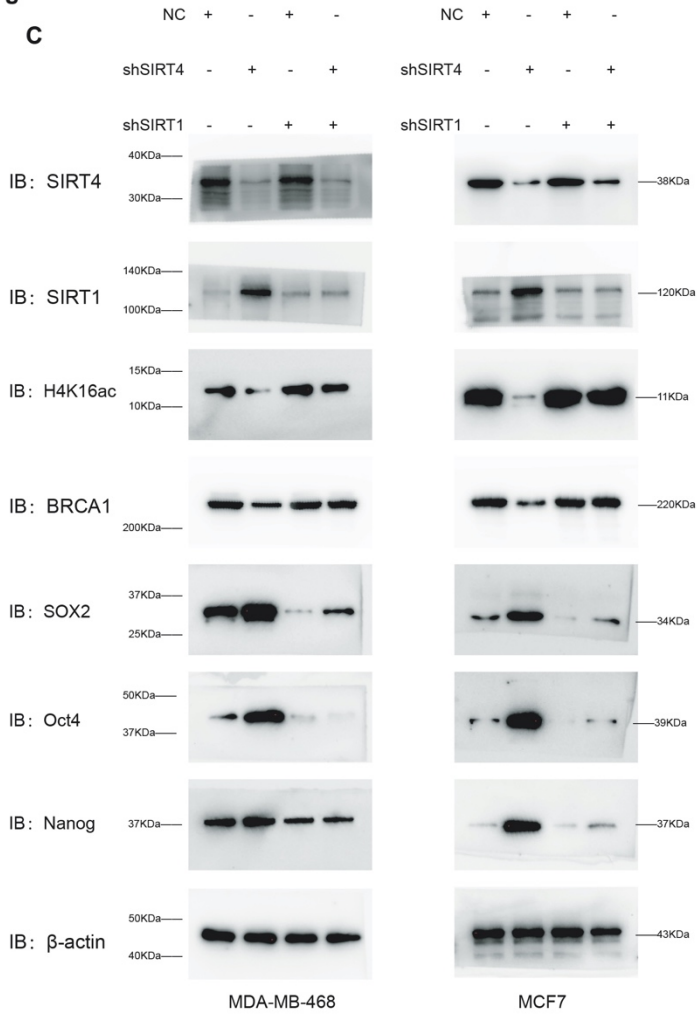
Fig 5**Fig 7**

Fig 6

C



sFig 2

A

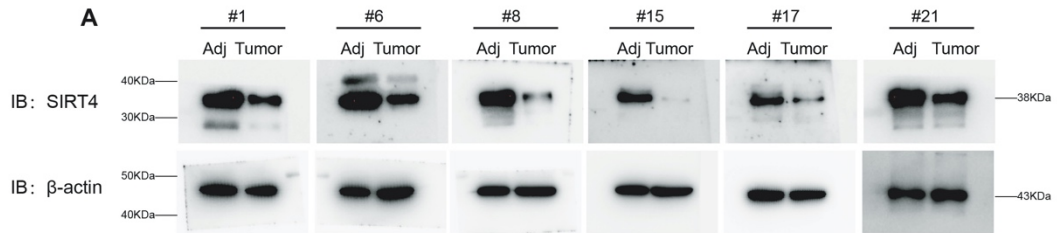
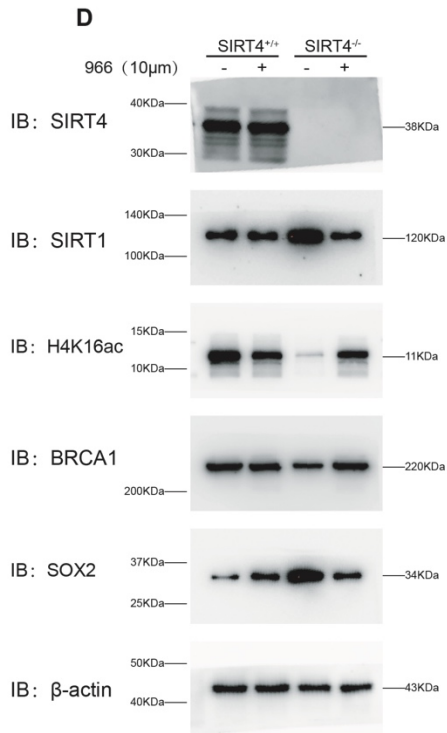
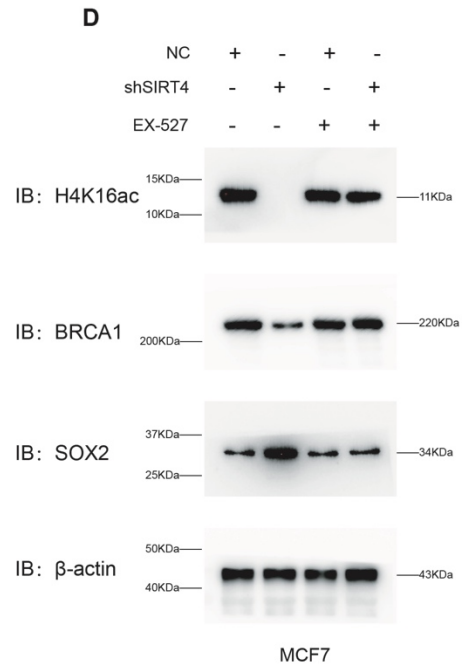
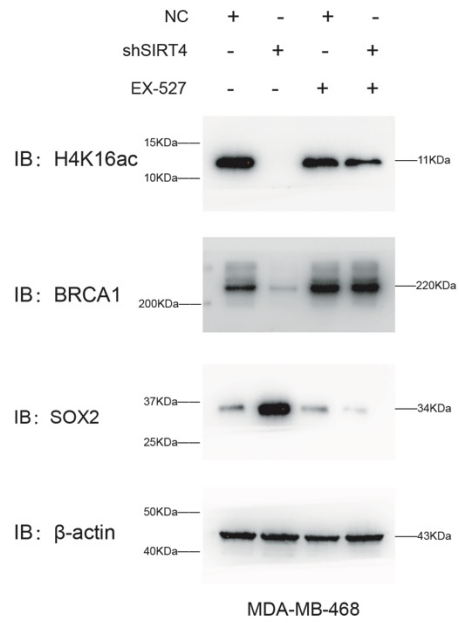
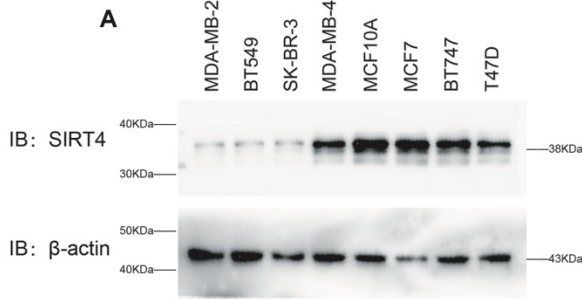
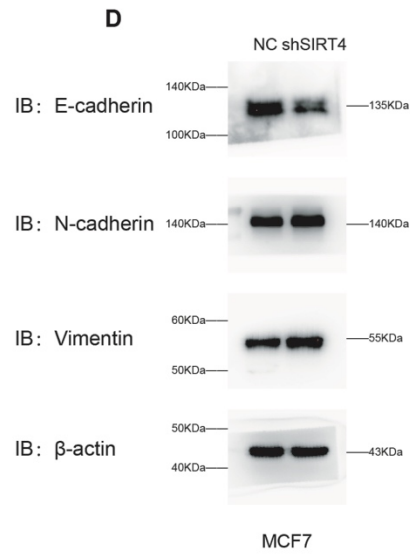
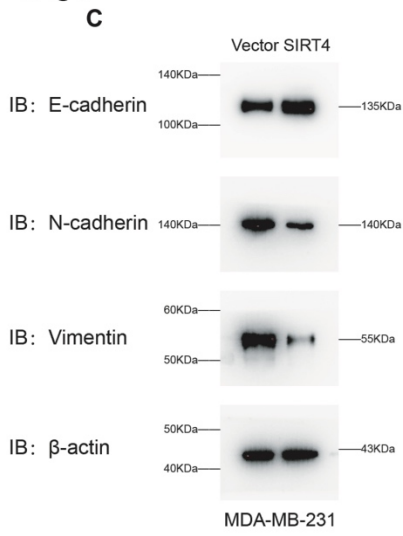
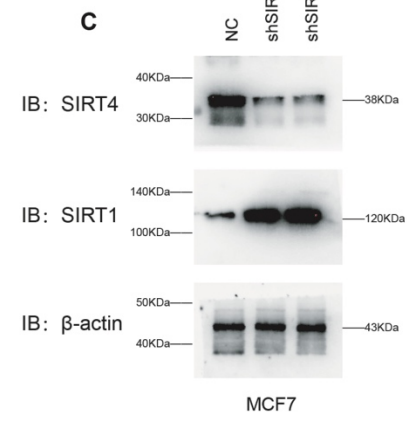
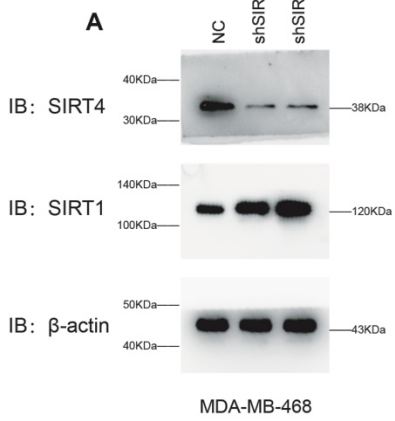


Fig 7**Fig 8****sFig6**

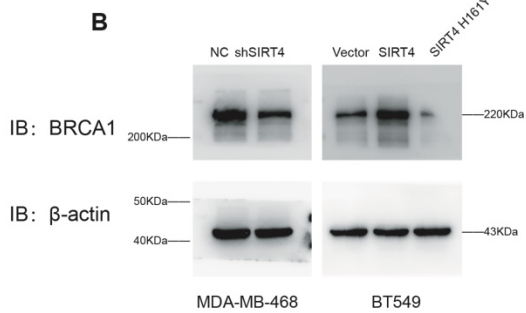
sFig 8



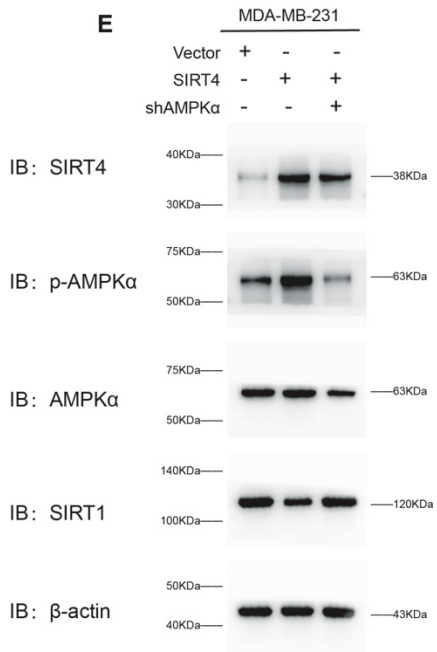
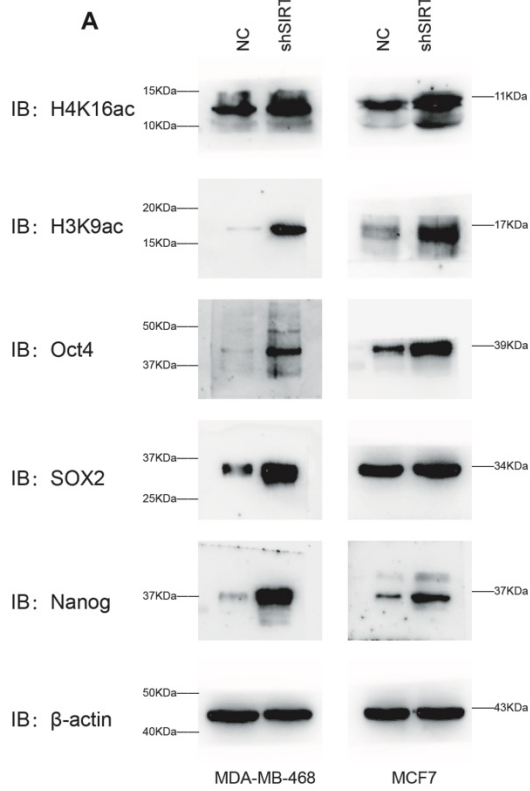
sFig 9



sFig 12



sFig 11



sFig 15

